water

MDPI

Article

Optimization Study of the Structural Parameters of an Artificial Percolation Intake Riverbed Based on a Numerical Orthogonal Test

Ming Yang [1], Lianle Wang [1,2], Xihuan Sun [1,*], Yongye Li [1] and Lijian Zheng [1]

[1] College of Water Resources Science and Engineering, Taiyuan University of Technology, Taiyuan 030024, China; yangm_0018@163.com (M.Y.); lianlewang@163.com (L.W.); liyongye@tyut.edu.cn (Y.L.); zhenglijian@tyut.edu.cn (L.Z.)
[2] China Railway 18th Bureau Group Co., Ltd., Tianjin 300000, China
* Correspondence: sunxihuan@tyut.edu.cn; Tel.: +86-135-1360-0012

Abstract: Research on water abstraction techniques in sandy rivers is crucial for addressing water scarcity issues in northern China. This study introduces an artificial percolation water intake riverbed structural model designed to prevent sand intake and facilitate the extraction of clear water from sandy rivers, the main function of which is to artificially construct a helical flow field to realize the separation of water and sand and, at the same time, percolate the water. In this paper, we use a numerical orthogonal test method to study the influence of structural parameters and their combinations on water extraction by percolation, and the preferred combination of structural parameters. The main conclusions of this paper are as follows: Under the condition of certain structural parameters of the artificial riverbed, the single-width flow rate has an important effect on the mean circumferential flow rate of the vortex tube and the vortex tube seepage volume. The effect of different structural parameters on the mean circumferential flow rate of the vortex tube and the vortex tube seepage varies in magnitude. The longitudinal slope of artificial riverbed i had the greatest and most significant effect on the mean circumferential flow rate of the vortex tube, and each structural parameter had some effect on the vortex tube seepage Q but not to a significant level. When the sand content of the water flow is 15 kg/m^3 and the maximum sand grain size of the suspended mass is 2 mm, the optimal structural parameter combinations of the artificial riverbed under different working conditions are as follows: Combination 20 is the optimal structural parameter combination for q = 0.3 m^2/s; Combination 24 is the optimal structural parameter combination for q = 0.6 m^2/s; and Combination 24 is the optimal structural parameter combination for q = 0.9 m^2/s. The present study is of great significance for understanding the influence of each structural parameter and its combination on the effect of the water intake and sand discharge of an artificial percolation intake riverbed, and for optimizing the combination of the structural parameters of an artificial percolation intake riverbed.

Keywords: orthogonal test; range analysis; artificial percolation intake riverbed; infiltration vortex tube

check for updates

Citation: Yang, M.; Wang, L.; Sun, X.; Li, Y.; Zheng, L. Optimization Study of the Structural Parameters of an Artificial Percolation Intake Riverbed Based on a Numerical Orthogonal Test. *Water* **2024**, *16*, 3110. https://doi.org/10.3390/w16213110

Academic Editor: Bommanna Krishnappan

Received: 2 October 2024
Revised: 17 October 2024
Accepted: 28 October 2024
Published: 30 October 2024

Copyright: © 2024 by the authors. Licensee MDPI, Basel, Switzerland. This article is an open access article distributed under the terms and conditions of the Creative Commons Attribution (CC BY) license (https://creativecommons.org/licenses/by/4.0/).

1. Introduction

1.1. Research Background

There is a severe water shortage in northern China. The high concentration of sand and the fine grain size of the sand make it very difficult to handle, so there is an increasing shortage of water resources available in the sandy rivers of northern China. The current water extraction and desanding techniques for sandy rivers mainly include the following four methods: (1) Seepage water extraction occurs through special geological formations and head differences, e.g., the interception of submerged flow technology or underground

seepage technology [1,2]. (2) Hydrocyclone technology uses artificially constructed hydrocyclone fields and the different densities of water to separate them, e.g., hydrocyclones, sand discharge vortex tubes [3,4], and cyclone sand channels [5]. (3) The physical properties of sediment are used to construct equipment for water–sediment separation. For example, sand sedimentation tanks [6], the separation of gills [7], physical adsorption [8], and multi-dune models are commonly used in sewage treatment engineering [9,10]. (4) Reverse osmosis is realized under pressure using membrane separation technology, which relies on the function of permeable/semi-permeable membranes [11]. A commonly used reverse osmosis water purifier is the sand sedimentation tank; however, it covers a large area, requires a large investment, and has high operation costs in the later stages. Additionally, separation gills need hydrostatic sedimentation and have low separation efficiency [12]. In seepage water intake methods, such as seepage wells and seepage canals, the filter material is prone to silt accumulation, making it difficult to ensure a sufficient amount of water intake. Reverse osmosis membranes need a high inlet head and have high energy consumption and operating costs. Finally, physical adsorption methods have the disadvantages of low adsorption efficiency and high costs of the adsorption treatment materials, among other shortcomings.

Compared to other methods, the construction of hydraulic cyclone fields has the advantages of a strong processing capacity and occupation of a small area. Additionally, they can treat water flows with high sand content highly efficiently, and they are very widely used for water extraction and desanding. Domestic and foreign scholars have conducted a series of studies on cyclone field technology for water and sand separation. Fan [13], Wang [14], Atkinson E. [15,16], and Zhang et al. [17] have determined the reasons for the formation of a spiral flow in vortex tubes for sand discharge, the sand discharge effect, and its influencing factors by means of flume tests. Zhao [18], Li [19], and Mohammad [20] combined physical tests and numerical simulations to study the flow field characteristics, sediment trajectory, and water–sand separation efficiency of turbid water hydraulic separation devices. Zhang [21] and Cui [22] used numerical analysis, physical tests, and other methods to study the internal fluid motion law of hydrocyclones and the trajectory of particles in the flow field. Hydrocyclones are widely used in many fields, such as water conservancy, mining, and municipal engineering. Li [23] studied sand discharge funnels and have proposed sand discharge funnel optimization schemes. Nan [24,25] carried out systematic research on the hydraulic characteristics, sand discharge characteristics, and sand discharge effects of cyclone sand discharge channels. However, the above cyclone field technologies for water and sand separation have certain limitations. For example, in the vortex tube method, the sand separation effect is very limited, silt accumulates easily, and it consumes a large amount of water; hydrocyclones are not good for the separation of fine particles of sand; and sand funnels easily lead to clogging problems.

In response to the existing challenges associated with water intake from sandy rivers, the authors suggest an artificial percolation riverbed water intake structure to facilitate a water intake technique that selectively extracts water without capturing sand during the diversion process from a sandy river. The artificial percolation water intake riverbed consists of a bed with percolation vortex tubes on both sides and a sediment transport flume in the center, the arrangement of which is shown in Figure 1 [26].

However, as a new method of water intake from sandy rivers, the key issue is how to rationally set the structural parameters of the artificial percolation riverbed to realize the separation of water and sand, and to facilitate sand transport. The artificial percolation water intake riverbed structure involves multiple structural parameters and, at present, for the optimization design of different structures with multiple parameters, the most widely used is the orthogonal test method [27]. The core of the orthogonal test method lies in "orthogonality"; orthogonality means that the pairing of different combinations of levels of any two factors is homogeneous in the designed test protocol. This means that each level of each factor has the opportunity to be combined with each level of the other factors an equal number of times. This allows enough information to be obtained to analyze

the extent to which each factor affects the outcome of the test with a smaller number of trials. Therefore, compared with the traditional enumeration method, which is laborious, time-consuming, and inefficient, the orthogonal test method can significantly reduce the number of tests and workload [28]. For example, Yuqin Wang [29] carried out a multi-parameter optimization design for centrifugal pumps using orthogonal tests and verified the accuracy of the optimization based on the tests. Jinbao Chen [30] optimized the turbine runner geometry parameters based on an orthogonal test method and CFD to improve the efficiency. Fang Liu [31] used an orthogonal experimental design to optimize the twisted nose crest configuration of the spillway of the Na Zi Xia project, and the optimal body shape was obtained. Chen Zhang [32] conducted a hydraulic optimization study of a lateral intake pumping station using an orthogonal experimental method. Zhenhua Shen [33] conducted numerical tests on the cavitation characteristics of water pumps based on orthogonal tests, and finally obtained a numerical model related to the cavitation characteristics of water pumps. Therefore, for the optimization study of different combinations of structural parameters of the artificial percolation water intake riverbed, the orthogonal test method can greatly reduce the number of experiments under the premise of ensuring the validity of the test results.

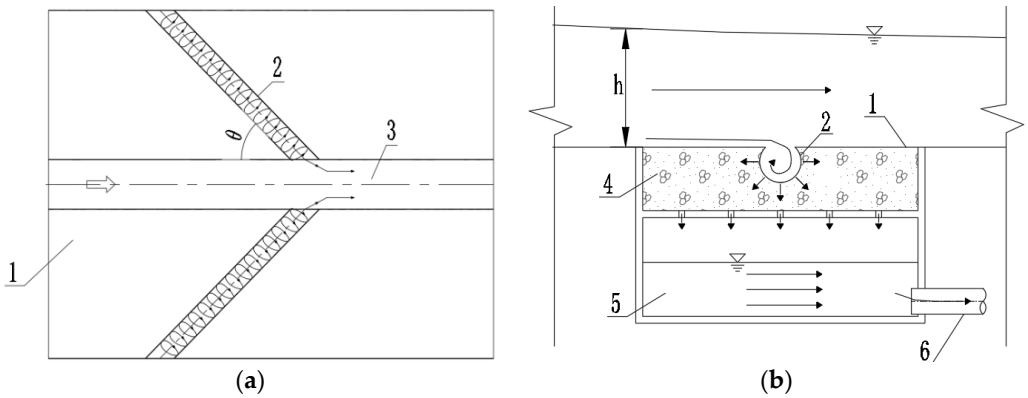


Figure 1. (**a**) Schematic of artificial percolation riverbed; (**b**) schematic of artificial percolation riverbed profile. (1) Artificial percolation; (2) percolation vortex tube; (3) sediment transport flume; (4) anti-filtration material; (5) catchment area; (6) water duct.

Based on physical tests and numerical simulations, this paper adopts a numerical orthogonal test method to determine the combination of structural parameters of the artificial percolation water intake riverbed, and takes the vortex tube average circumferential flow rate and seepage volume as the optimization indexes, and carries out numerical simulation research on the hydraulic characteristics of the water intake structure of the artificial percolation water intake riverbed, so as to analyze the impacts of the structural parameters of the artificial percolation water intake riverbed and their combinations on the optimization indexes under different working conditions. Extreme difference analysis is used to analyze the influence of each structural parameter and its combination on the optimization index under different working conditions, and different combinations of structural parameters under different working conditions are discriminated under the conditions of a certain amount of sand content in the water flow and the maximum sand particle size, and finally the optimal combination of structural parameters of the artificial percolation water intake riverbed under different working conditions that can achieve better water intake effect and also have better sand discharge capacity is summarized.

1.2. Description of the Structural Parameters of the Artificial Percolation Water Intake Riverbed

The structural parameters of the artificial percolation water intake riverbed include the longitudinal slope of artificial riverbed i, the transverse slope i_h, the ratio of the width of the sediment transport flume b_z to the width of the beach b_t in the artificial riverbed $W_b = b_z/b_t$, the ratio of the percolation vortex tube diameter D to h_s (difference in elevation

between the bottom of the sediment transport flume and the bottom of the vortex tube and sediment transport flume joint) $W_g = D/h_s$, the angle θ between the axis of the percolation vortex tube and the main stream of the artificial riverbed, the opening holes' ratio Ω of the percolation vortex tube, the opening angle α of the percolation vortex tube, etc. [15,16]. Figure 2 shows a schematic diagram of the parameters.

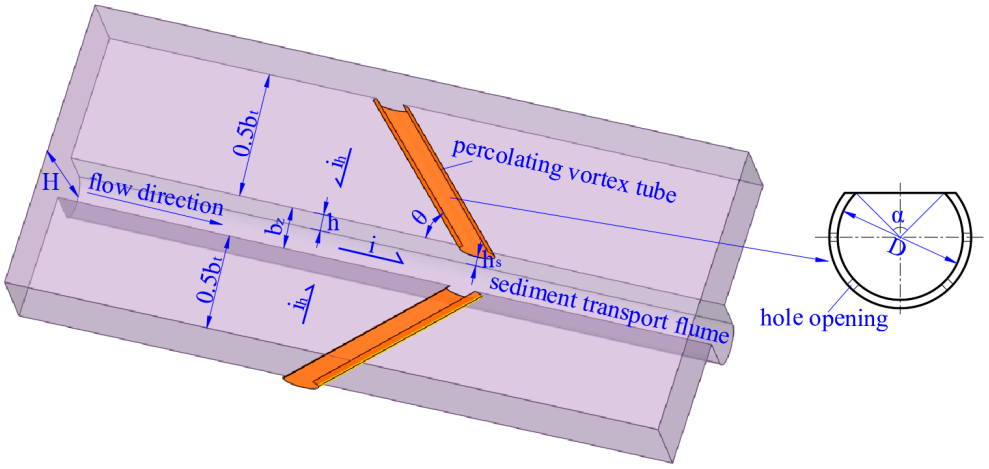


Figure 2. Schematic diagram of the parameters of the riverbed for artificial percolation water intake. H is the water depth of the artificial percolation intake riverbed, and h is the water depth of the sediment transport flume.

Here, longitudinal slope i of the artificial riverbed directly affects the size of the mainstream flow rate in the artificial infiltration intake riverbed, and the transverse slope ih affects the mainstream flow rate in the artificial infiltration intake riverbed at the same time as it affects the flow rate in the artificial infiltration intake riverbed in the longitudinal direction perpendicular to the distribution of the secondary flow in the open channel [34]. The artificial percolation intake riverbed is a compound section, and the ratio of the widths of the sediment transport flume and the beach, W_b, affects the flow ratio of the artificial riverbed conveyor and the beach, as well as the flow velocity distribution in the artificial riverbed section, and also affects the length of the percolation vortex tubes, the slope of the axial direction of the percolation vortex tubes, and the total area of the percolation holes. The ratio W_g of the diameter D of the infiltration vortex tube to h_s will affect the velocity distribution at the junction of the vortex tube and the sediment transport flume. The angle θ between the percolation vortex tube axis and the main stream of the artificial riverbed affects the component of the main stream flow velocity at the vortex tube axis and perpendicular to the vortex tube axis, as well as determining the length of the vortex tube axis, which in turn affects the size of the total vortex tube percolation holes' area. The larger the percolation vortex tube opening Ω and the larger the total area of the percolation holes, the greater the amount of water that can percolate. The opening angle α of the percolation vortex tube affects the diversion ratio in the percolation vortex tube as well as the velocity component of the water flow at the inlet of the vortex tube.

2. Numerical Modeling and Experimental Validation

2.1. Geometric Modeling and Meshing

The dimensions of the geometric model created for this study and the coordinate arrangement are shown in Figure 3 [26]. The unit of measurement for all dimensions in the figure is millimeter (mm). The artificial riverbed has a single-width flow q of 0.06 m^2/s, i equal to 5/1000, i_h equal to 1/100, W_h equal to 1/2.5, W_b equal to 1/6, W_g equal to 1/2, θ equal to 45°, Ω equal to 1.4%, and α equal to 90°. The model is meshed using Polyhedra mesh in Ansys (Version 2022R1) Meshing. The number of grids is 2.9 million.

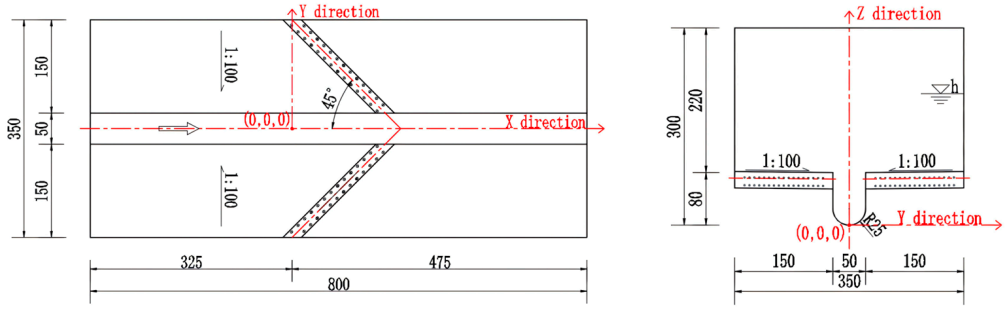


Figure 3. Dimensions and coordinate arrangement of the geometric model of the artificial percolation riverbed.

2.2. Control Equations

In this simulation, the Volume of Fluid (VOF) model is employed to calculate the behavior of the liquid–gas two-phase flow. To accurately capture the viscous effects, the realizable k-ε model is chosen as the viscous model. The finite volume method is utilized to iteratively solve the governing equations in a hidden format. The velocity–pressure coupling is achieved through the coupled algorithm. The QUICK format is employed as the discrete format for the numerical solution. Additionally, the Enhanced Wall Treatment wall function is utilized to account for boundary effects.

2.3. Model Validation

In order to verify the reliability of the numerical simulation, a physical model test is required to compare the numerical simulation results, and the layout of the test system is shown in Figure 4.

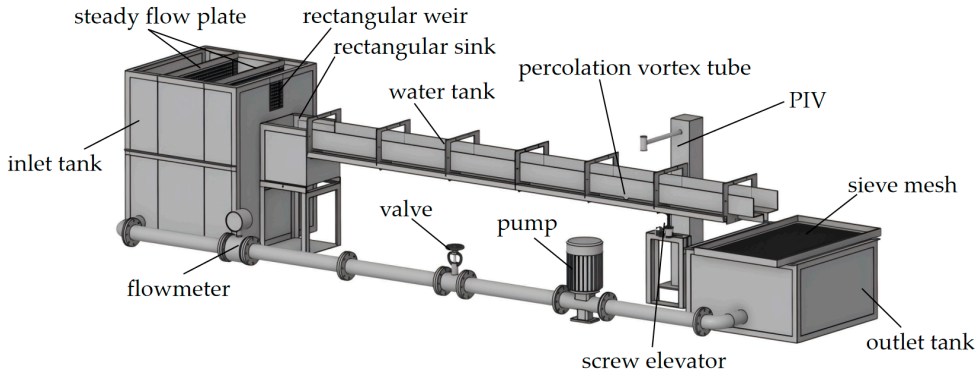


Figure 4. Physical test setup diagram.

During the test, the inlet and outlet tanks were filled with water and tracer particles were added for data acquisition by the particle image velocimeter. A centrifugal pump was activated to circulate the water through the test setup, and the flow of water through the pipeline was adjusted to the required Reynolds number for the test by controlling the valves and observing the electromagnetic flowmeter readings. The test section was photographed using a Particle Image Velocimetry (PIV) (Dantec Dynamics A/S, Copenhagen, Denmark) after the flow was stabilized. PIV primarily employs a pulsed laser light source to illuminate a designated test section of the water flow that includes tracer particles. Subsequently, a high-speed camera captured particle images at two distinct time points, enabling the calculation of particle displacements using specific algorithms to determine the velocity of the water flow. This method offers numerous advantages, such as non-invasive, full-field, and high-precision measurements. When filming, the outer wall opening of the percolation vortex tube was first closed with waterproof tape, and the section of the test section was filmed, then the outer wall opening of the percolation vortex tube was opened, and then filmed again, while measuring the change in the water level in the catchment tank within a

certain period of time, in order to calculate the amount of water seepage. The results were processed by PIV post-processing software (Dynamic Studio 5.0) to obtain the required flow rate values.

Comparative analyses of simulated and experimental values of the velocity along the flow direction of the measured line between the profile measurement point (0, 0.065, 0.085) and the measurement point (0.120, 0.065, 0.085) in the sediment transport flume were carried out, respectively. Comparison charts are shown in Figures 5 and 6. According to the comparison charts, it can be seen that the simulated values fit well with their corresponding experimental values, and the maximum deviation of the flow rate is not more than 2.2%, which proves the reliability of this numerical simulation; the numerical simulation can be carried out for each design condition and the flow analysis can be carried out accordingly.

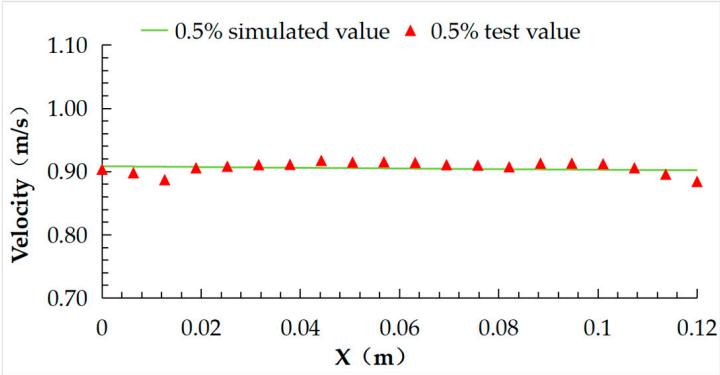


Figure 5. Comparison of simulated and experimental values of flow velocity in an artificial non-percolation riverbed.

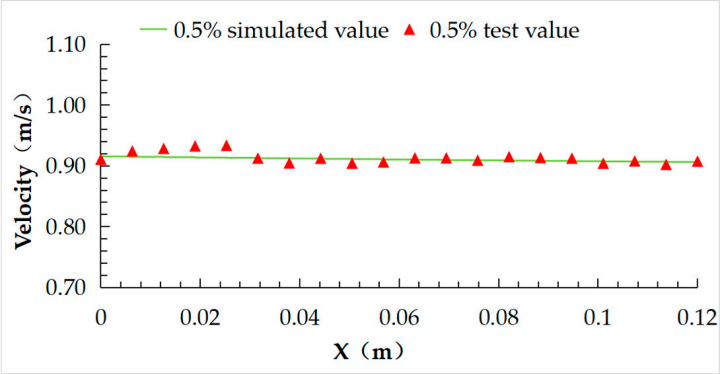


Figure 6. Comparison of simulated and experimental values of flow velocity in an artificial percolation riverbed.

3. Orthogonal Experimental Design

The vortex tube mean circumferential flow velocity V_r and infiltration vortex tube seepage Q [35] are key measures of water withdrawal and sand removal from artificial infiltration intake riverbeds. The greater the average circumferential flow velocity V_r of the percolation vortex tube, the more favorable it is for sediment initiation and suspension to avoid sediment deposition in the vortex tube. And under the same conditions, the larger the amount of seepage Q is, the larger the amount of water extracted from the riverbed by artificial percolation, and the greater the economic benefits. However, the variation of seepage volume will inevitably affect the magnitude of the mean circumferential flow rate in the vortex tube. Therefore, the aim of this study is to achieve maximum water seepage while obtaining the largest possible mean circumferential flow rate in the vortex tube. Therefore, V_r as well as Q are used as optimization indexes for this experiment. The influencing parameters include the artificial riverbed structural parameters such as i, i_h, W_b, W_g, θ, Ω,

α, and the incoming flow conditions such as the single-width flow rate, q. According to Section 1.1, these structural parameters have different degrees of influence on the flow field distribution and the amount of seepage of the artificial percolation riverbed, which in turn affect the effect of water extraction and sand removal in the artificial percolation riverbed. Therefore, an in-depth study of these structural parameters is needed. However, due to the large number of levels of structural parameters, orthogonal tests were used for the optimization of the parameters of the artificial percolation water intake riverbed in order to ensure the accuracy of the numerical tests as well as to reduce the workload. According to the results of previous research [36], the vortex tube opening angle α was set to 90°. The remaining six factors i, i_h, W_b, W_g, θ, and Ω, which we denote by J, K, L, M, N, and O, respectively, were designed with five levels for each factor, as shown in Table 1, and the orthogonal test table L25 (5^6) was used to generate 25 sets of test combination schemes for the structural parameters of the artificial riverbed, as shown in Table 2.

Table 1. Parameters and levels.

Parameter Level	i	i_h	W_b	W_g	Θ (°)	Ω
	J	K	L	M	N	O
1	0.01	0.01	0.10	0.25	15	5
2	0.02	0.02	0.20	0.50	30	10
3	0.04	0.04	0.40	1	45	15
4	0.08	0.08	0.80	2	60	20
5	0.16	0.16	1.00	4	75	25

Table 2. Structural parameter combination test program.

No.	Parameter Combination	No.	Parameter Combination	No.	Parameter Combination	No.	Parameter Combination	No.	Parameter Combination
1	$J_1K_1L_1M_1N_1O_1$	6	$J_2K_1L_2M_3N_4O_5$	11	$J_3K_1L_3M_5N_2O_4$	16	$J_4K_1L_4M_2N_5O_3$	21	$J_5K_1L_5M_4N_3O_2$
2	$J_1K_2L_2M_2N_2O_2$	7	$J_2K_2L_3M_4N_5O_1$	12	$J_3K_2L_4M_1N_3O_5$	17	$J_4K_2L_5M_3N_1O_4$	22	$J_5K_2L_1M_5N_4O_3$
3	$J_1K_3L_3M_3N_3O_3$	8	$J_2K_3L_4M_5N_1O_2$	13	$J_3K_3L_5M_2N_4O_1$	18	$J_4K_3L_1M_4N_2O_5$	23	$J_5K_3L_2M_1N_5O_4$
4	$J_1K_4L_4M_4N_4O_4$	9	$J_2K_4L_5M_1N_2O_3$	14	$J_3K_4L_1M_3N_5O_2$	19	$J_4K_4L_2M_5N_3O_1$	24	$J_5K_4L_3M_2N_1O_5$
5	$J_1K_5L_5M_5N_5O_5$	10	$J_2K_5L_1M_2N_3O_4$	15	$J_3K_5L_2M_4N_1O_3$	20	$J_4K_5L_3M_1N_4O_2$	25	$J_5K_5L_4M_3N_2O_1$

4. Analysis of Orthogonal Test Results

According to the test scheme in Table 2, the single-width flow rates designed in this study are 0.3 m^2/s, 0.6 m^2/s, and 0.9 m^2/s. The following is a sequential study of the effects of different combinations of artificial percolation intake riverbed structural parameters on the average circumferential flow rate of percolation vortex tubes, V_r, and the amount of seepage, Q, for different single-width flow rates, and the results of the study are shown in Figure 7.

The following can be seen from the results of the orthogonal test in Figure 7:

1. From Figure 7a, it can be seen that the combination of structural parameters has an important effect on the mean circumferential flow velocity of the vortex tube. Different combination numbers represent different combinations of structural parameters, and each combination number presents different vortex tube mean circumferential flow velocities, with Combination 5 having the smallest vortex tube mean circumferential flow velocity and Combination 24 having the largest vortex tube mean circumferential flow velocity. It can also be seen that the single-width flow rate has an important effect on the mean circumferential flow rate of the vortex tube, which increases sequentially as the single-width flow rate increases from 0.3 m^2/s to 0.6 m^2/s and then to 0.9 m^2/s under a certain combination of structural parameters of the artificial riverbed. When

the single-width flow increases from 0.3 m^2/s to 0.6 m^2/s, the smallest increase is in Combination 15 with 15.2% and the largest increase is in Combination 5 with 57.4%. When the single-width flow rate increases from 0.6 m^2/s to 0.9 m^2/s, the smallest increase is in Combination 2 with 9.0% and the largest increase is in Combination 5 with 48.5%. It can be seen that the increase in flow rate will lead to an increase in the vortex tube mean circumferential flow rate; this is because with the increase in flow rate, the Reynolds number corresponding to the vortex tube flow field will also increase, the overall flow rate of the vortex tube flow field will increase, and the corresponding vortex tube mean circumferential flow rate will also increase.

2. From Figure 7b, it can be seen that the combination of structural parameters has an important effect on the amount of water seepage. All combination numbers show different water seepages, with the smallest seepage at Combination 5 and the largest seepage at Combination 24. It can also be seen that the single-width flow rate has an important effect on the seepage volume, and the vortex tube seepage volume increases sequentially when the single-width flow rate increases from 0.3 m^2/s to 0.6 m^2/s and then to 0.9 m^2/s under the condition of a certain structural parameter of the artificial riverbed. When the single-width flow increases from 0.3 m^2/s to 0.6 m^2/s, the smallest increase is in Combination 7 with 15.9% and the largest increase is in Combination 5 with 47.8%. When the single-width flow increases from 0.6 m^2/s to 0.9 m^2/s, the smallest increase is in Combination 23 with 9.3% and the largest increase is in Combination 16 with 30.9%. It can be seen that an increase in flow rate will lead to an increase in vortex tube seepage; this is because with the increase in flow rate and the overall rise in the water level of the riverbed of the artificial percolation water intake, the vortex tube flow field corresponding to the pressure will also increase, and the vortex tube flow field pressure increase will lead to vortex tube seepage and an overall increase in the amount of water.

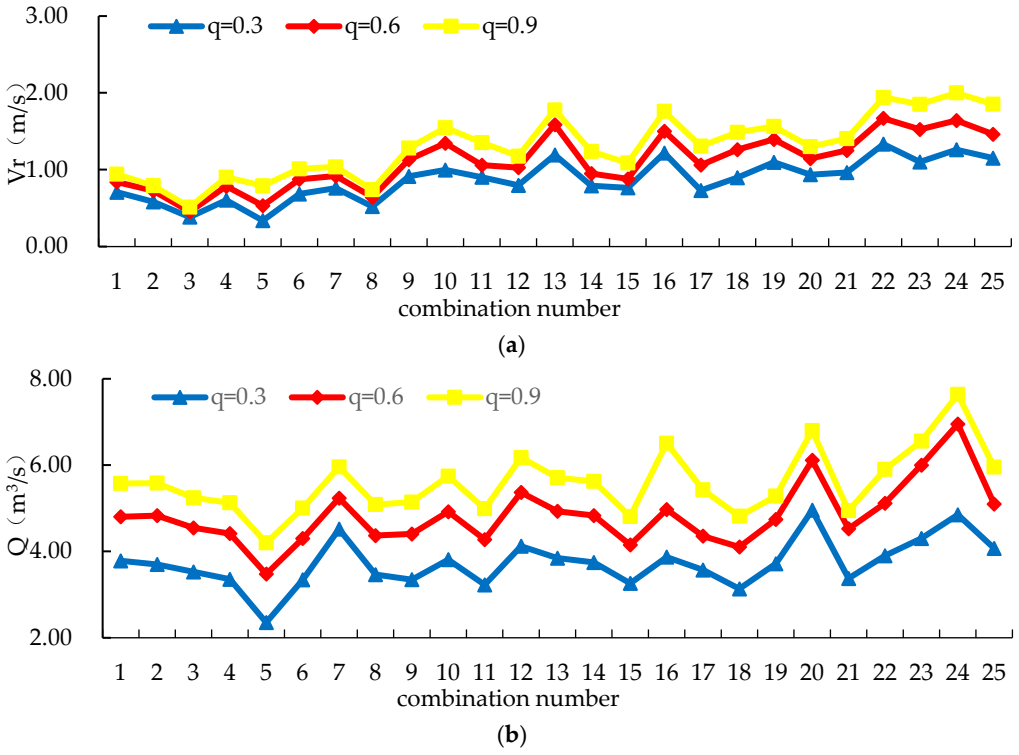


Figure 7. Orthogonal test results. (**a**) Mean circumferential flow velocity of vortex tubes Vr; (**b**) the amount of seepage Q.

5. Analysis of Test Results

5.1. Range Analysis

Range analysis is the difference between the maximum and minimum values in a set of data. In orthogonal tests, for each parameter, the degree of influence of the parameter on the test index can be measured by calculating the range of the test index at different levels of the parameter. In general, the range of the corresponding parameter under each test indicator is different, and the R_j mainly reflects the magnitude of the selected level under each parameter in terms of its influence weight on the test indicator. The larger the R_j, the greater the weight of the influence of the level selected under this parameter on the test indicator. Therefore, range analysis can help us to quickly identify the key factors, and then we can prioritize the adjustment of the factors that have a greater impact on the results, so that we can obtain the greatest improvement in the results with the smallest input. The range R_j is calculated by the following formula.

$$\overline{X_i} = \frac{1}{N_i} X_i \tag{1}$$

$$R_j = max\left(\overline{X_1}, \overline{X_2}, \ldots \overline{X_i}\right)\ min\left(\overline{X_1}, \overline{X_2}, \ldots \overline{X_i}\right) \tag{2}$$

X_i and $\overline{X_i}$ (i = 1, 2, 3…) denote the sum of the values of each parameter i level and the average of each parameter i level, respectively.

Based on the numerical simulation results, Figure 7, we sequentially performed an range analysis of the role of different structural parameters on the mean circumferential flow rate of the vortex tube and the vortex tube seepage in the artificial riverbed. Table 3 shows the table of the range analysis of different structural parameters for the q = 0.3 m^2/s condition. Table 4 shows the table of the range analysis of different structural parameters for the q = 0.6 m^2/s condition. Table 5 shows the table of the range analysis of different structural parameters for the q = 0.9 m^2/s condition. The five levels in the table correspond to the mean values of the vortex tube mean circumferential flow velocity and vortex tube water seepage for different structural parameters at this level. R_j is the extreme deviation of the different structural parameters, which is equal to the maximum minus the minimum of the mean values at the five levels. The results are then sorted according to the magnitude of the extreme deviation, and the last row is the ranking result.

1. From the above table, it can be seen that the influence of different structural parameters on the vortex tube average circumferential flow velocity V_r has different weights; according to the results of the range analysis, the influence of the primary and secondary order according to the size of the R_j is ranked. The main order of influence of different structural parameters on the V_r of the vortex tube is as follows: J > N > L > M > K. And the parameter O affects the vortex tube mean circumferential flow velocity V_r in a different order of priority under different flow conditions. When the q is 0.3 m^2/s and 0.6 m^2/s, the parameter O affects the V_r in the order of J > N> L > O > M > K. When the q is 0.9 m^2/s, the parameter O affects the vortex tube mean circumferential flow velocity V_r in the order of J > N > L > M > O > K.
2. From the above table, it can be seen that different structural parameters have different weights and sizes of influence on the vortex tube seepage Q. According to the results of the range analysis, the order of influence is ranked according to the size of the R_j. The more influential parameter is parameter M, and the less influential parameter is parameter O. The different structural parameters have a different order of influence on the vortex tube seepage under different flow conditions. When the q is 0.3 m^2/s, the main order of influence of different structural parameters on the vortex tube seepage Q in terms of the magnitude of the range is M > N >J > K > L > O. When the q is 0.6 m^2/s, the effects of different structural parameters on Q are in the following order of precedence: J > M > N > K > O > L. When the q is 0.9 m^2/s, the effects of different structural parameters on Q are in the following order of precedence: M > L > K > J> O

> N. Therefore, it can be seen that with the change in flow conditions, the influence of different structural parameters on the vortex tube seepage Q varies greatly in the order of magnitude.

Table 3. q = 0.3 m^2/s range analysis table for different structural parameters.

Level	V_r (m/s)						Q (m^3/s)					
	J	K	L	M	N	O	J	K	L	M	N	O
1	0.52	0.89	0.98	0.94	0.89	0.80	3.34	3.52	3.99	3.67	4.10	3.79
2	0.77	0.84	0.76	0.85	1.05	0.89	3.70	3.96	3.85	3.66	4.01	3.49
3	0.89	0.82	0.92	0.85	0.75	0.85	3.64	3.65	3.58	4.22	3.65	3.71
4	0.97	0.93	0.87	0.86	0.80	0.95	3.85	3.80	3.65	3.78	3.53	3.88
5	1.16	0.84	0.79	0.83	0.84	0.84	4.10	3.69	3.56	3.30	3.33	3.76
R_j	0.64	0.11	0.22	0.12	0.30	0.15	0.76	0.44	0.43	0.92	0.77	0.39
rank	1	6	3	5	2	4	3	4	5	1	2	6

Table 4. q = 0.6 m^2/s range analysis table for different structural parameters.

Level	V_r (m/s)						Q (m^3/s)					
	J	K	L	M	N	O	J	K	L	M	N	O
1	0.67	1.10	1.24	1.21	1.13	1.01	4.41	4.58	4.96	4.76	5.34	4.93
2	0.98	1.08	0.94	1.08	1.36	1.13	4.65	4.98	4.93	4.80	5.32	4.54
3	1.10	1.09	1.13	1.04	0.96	1.09	4.71	4.79	4.64	5.42	4.63	4.82
4	1.27	1.18	1.15	1.08	1.02	1.21	4.86	5.07	4.79	4.84	4.49	4.97
5	1.51	1.07	1.07	1.11	1.06	1.08	5.54	4.75	4.84	4.34	4.40	4.90
R_j	0.84	0.11	0.30	0.17	0.40	0.20	1.12	0.49	0.32	1.09	0.94	0.43
rank	1	6	3	5	2	4	1	4	6	2	3	5

Table 5. q = 0.9 m^2/s range analysis table for different structural parameters.

Level	V_r (m/s)						Q (m^3/s)					
	J	K	L	M	N	O	J	K	L	M	N	O
1	0.79	1.29	1.43	1.43	1.31	1.21	5.51	5.29	5.77	5.32	5.59	5.30
2	1.12	1.25	1.09	1.26	1.57	1.35	5.11	5.35	5.00	6.06	5.59	5.28
3	1.33	1.27	1.32	1.24	1.18	1.24	5.43	5.36	5.48	5.17	5.40	5.53
4	1.48	1.40	1.39	1.29	1.18	1.39	5.62	5.40	5.81	5.31	5.30	5.45
5	1.81	1.31	1.29	1.31	1.28	1.33	5.55	5.81	5.14	5.35	5.33	5.64
R_j	1.02	0.15	0.34	0.19	0.39	0.17	0.51	0.52	0.81	0.90	0.29	0.37
rank	1	6	3	4	2	5	4	3	2	1	6	5

5.2. Analysis of Variance

Compared to range analysis, ANOVA takes into account the effect of fluctuations in the data of a parameter on the overall results, provides criteria for judging the significance of the parameter, and complements range analysis with mutual validation. So, we used a one-way ANOVA and Tukey's HSD to test the significance of the differences in the effects of different structural parameters on the mean circumferential flow rate of the vortex tubes and the vortex tube seepage volume. Differences were considered significant at $p < 0.05$ [37].

Therefore, based on the results of the ANOVA, it is possible to determine which factors have a real impact on the results and which ones can be ignored, so that the design can be targeted for optimization and efficiency. The variance analysis was performed using Minitab (Version 22).

According to the numerical simulation results in Figure 7, we sequentially analyzed the ANOVA of the role of different structural parameters on the average circumferential flow rate V_r of the vortex tube and the vortex tube seepage volume Q in the riverbed of the artificial percolation intake, and the results are shown in Table 6.

Table 6. ANOVA table.

q (m^2/s)	Level	J	K	L	M	N	O
0.3	P (Vr)	0.001	0.967	0.713	0.971	0.467	0.934
	P (Q)	0.302	0.806	0.734	0.128	0.136	0.881
0.6	P (Vr)	0.002	0.992	0.768	0.963	0.442	0.943
	P (Q)	0.129	0.859	0.967	0.219	0.071	0.908
0.9	P (Vr)	0.004	0.988	0.765	0.965	0.586	0.966
	P (Q)	0.681	0.637	0.066	0.081	0.897	0.855

1. As can be seen from Table 6, according to the ANOVA, when the V_r is used as the optimization index, each structural parameter has different degrees of influence on the V_r. Among them, the *p*-value of parameter J is less than 0.05 under different working conditions, so parameter J has a significant effect on the V_r. The *p*-values of the remaining five parameters are all greater than 0.05, which shows that the parameters K, L, M, N, and O have different degrees of influence on the vortex tube mean circumferential flow velocity V_r, but they do not reach the significant level. When the vortex tube seepage volume Q is used as the optimization index, each structural parameter has different degrees of influence on the Q. However, the *p*-value of each structural parameter is greater than 0.05, so it can be seen that the influence of each structural parameter on the Q does not reach a significant level.
2. As can be seen from Table 6, the degree of influence of different structural parameters on the V_r varies under different flow conditions. The size of the influence degree is ranked according to the *p*-value, and the smaller the *p*-value is, the more significant the influence is. Sorting the results by *p*-value, when the q is 0.3 m^2/s, the order of significance of the effect of different structural parameters on V_r is J > N > L > O > K > M. When the q is 0.6 m^2/s, the order of significance of the effect of different structural parameters on V_r is J > N > L > O > M > K. When the single-width flow rate q is 0.9 m^2/s, the order of significance of the effect of different structural parameters on V_r is J > N > L > M > O > K. It can be seen that the significance of the effect of O, M, and K parameters on V_r changes as the flow conditions change. The significance of the effect of each structural parameter on the vortex tube seepage Q is also different under different flow conditions. Sorting the results by *p*-value, when the q is 0.3 m^2/s, then the order of significance of the effect of different structural parameters on Q is M > N > J > K > L > O. When the q is 0.6 m^2/s, then the order of significance of the effect of different structural parameters on Q is N > J > M > K > O > L. When the q is 0.9 m^2/s, then the order of significance of the effect of different structural parameters on Q is L > M > K > J > O > N. It can be seen that as the flow conditions change, the significance of the effect of different structural parameters on the vortex tube seepage Q varies greatly.
3. As can be seen from the results of the range analysis in Section 5.1 and the ANOVA, the results of the range analysis and ANOVA are basically the same. Parameter i had the largest and most significant effect on the V_r. As i increases, the V_r gradually

increases. This is because as i increases, the flow velocity increases as a whole, and, therefore, the V_r also increases as a whole.

6. Selection of Optimal Structural Parameters Under Certain Water Flow and Sand Content Conditions

6.1. Determination of the Sand Removal Effect

In the actual project, the river is mostly sandy water flow; water intake must consider the sand content of the water flow, the maximum sand particle size, and the corresponding water intake facilities' siltation problems. For the artificial percolation water intake riverbed structure proposed in this paper, the percolation vortex tube in the sediment does not silt; we can realize the percolation water intake and smooth sediment discharge. Therefore, the sand-holding force of the water flow in the riverbed of the artificial percolation water intake is greater than the sand content of the incoming water, and the average circumferential flow velocity V_r of the vortex tube is greater than the starting flow velocity of the largest sand grain size, which is the key index to determine whether the artificial riverbed is silted up during the water intake.

In this paper, the sand content of the water is 15 kg/m^3 and the maximum sand particle size of the suspended mass is 2 mm, which are the sand content working conditions to determine the sand discharge effect of the artificial percolation water intake riverbed. According to Fei's [38] suspended mass flow sand force Formula (3), we calculated the water flow sand force of different structural parameter combinations under different water flow conditions in the artificial percolation water intake riverbed, and the results are shown in Table 7. At the same time, according to Dou's [39] sediment starting flow rate Formula (4), we calculated that the maximum sand particle size of the suspended mass is 2 mm when the sediment starting flow rate needs to be more than 0.06 m/s.

$$S = 0.00265\left(\frac{U}{\omega_{90}}\right)^3\left(\frac{d_{90}}{R}\right)^{0.54} \tag{3}$$

where S is for the water flow sand force, kg/m^3; U is for the section of the average flow velocity, m/s; ω_{90} is for the sediment d_{90} sinking speed, m/s; d_{90} is for less than the size of the sediment particles accounted for, 90%, m; R is for the hydraulic radius, m.

$$\tau_c = k^2\rho\left(\frac{d'}{d_*}\right)^{1/3}\left[3.6\frac{\rho_s-\rho}{\rho}gd + \left(\frac{\gamma_0}{\gamma_{0*}}\right)^{5/2}\left(\frac{\varepsilon_0 + gh\delta\sqrt{\delta/d}}{d}\right)\right] \tag{4}$$

where τ_c is for the sediment starting flow rate, m/s; p is for the water density, kg/m^3; p_s is for the sediment density, kg/m^3; $k^2 = 0.0164$; $\varepsilon_0 = 0.15$ cm^3/s^2; $\delta = 2.31 \times 10^{-5}$ cm; h is for the depth; d is for the d_{50}; $d^* = 10$ mm; $d' = 2$ mm.

Table 7. Calculation table of sand-carrying force of water flow with different combinations of structural parameters in the artificial riverbed under different working conditions.

No. S (kg/m^3) q (m^2/s)	0.3	0.6	0.9
Combination 1	3.28	4.74	5.71
Combination 2	3.29	5.07	6.29
Combination 3	3.71	5.87	7.53
Combination 4	4.53	7.24	9.55
Combination 5	4.98	7.45	9.75
Combination 6	10.83	18.19	24.80
Combination 7	7.40	11.00	13.45

Table 7. *Cont.*

No. S (kg/m^3) q (m^2/s)	0.3	0.6	0.9
Combination 8	7.09	10.82	13.52
Combination 9	7.07	11.20	14.36
Combination 10	10.83	17.90	24.11
Combination 11	22.40	36.57	48.91
Combination 12	25.19	38.71	51.01
Combination 13	15.27	24.76	31.02
Combination 14	18.01	28.07	35.77
Combination 15	20.10	31.92	41.85
Combination 16	38.96	62.28	81.91
Combination 17	71.89	80.36	99.31
Combination 18	53.01	88.05	119.51
Combination 19	37.88	61.28	77.80
Combination 20	37.46	61.40	78.83
Combination 21	63.23	110.48	149.09
Combination 22	95.68	155.06	207.89
Combination 23	115.04	182.23	245.13
Combination 24	138.32	197.68	260.19
Combination 25	79.09	133.06	174.17

According to the sandy conditions, the artificial percolation water intake riverbed water flow sand force must be greater than 15 kg/m^3 and the vortex tube average circumferential flow velocity V_r must be greater than 0.06 m/s to remove combinations that do not meet the requirements for use of the combination of different conditions, as shown in Table 8.

Table 8. Statistical table of combinations of structural parameters that meet the requirements for use under different operating conditions.

No. S (kg/m^3) q (m^2/s)	0.3	0.6	0.9
Combination 6			24.80
Combination 10		17.90	24.11
Combination 11	22.40	36.57	48.91
Combination 12	25.19	38.71	51.01
Combination 13	15.27	24.76	31.02
Combination 14	18.01	28.07	35.77
Combination 15	20.10	31.92	41.85
Combination 16	38.96	62.28	81.91
Combination 17	71.89	80.36	99.31
Combination 18	53.01	88.05	119.51
Combination 19	37.88	61.28	77.80
Combination 20	37.46	61.40	78.83

Table 8. *Cont.*

No. S (kg/m^3) q (m^2/s)	0.3	0.6	0.9
Combination 21	63.23	110.48	149.09
Combination 22	95.68	155.06	207.89
Combination 23	115.04	182.23	245.13
Combination 24	138.32	197.68	260.19
Combination 25	79.09	133.06	174.17

6.2. Determination of Seepage

In order to meet the sand content of certain water flow conditions of the artificial riverbed water flow sand force and the vortex tube average circumferential flow velocity conditions, the larger the seepage must be, and the stronger the artificial riverbed water intake capacity, the better the effect of the water intake, and the greater the economic benefits. That is, to meet the preconditions at the same time, the greater the amount of water seepage must be; by analyzing Table 9, the requirements for the use of the structural parameters of the combination of water seepage statistics table can be obtained: under the q = 0.3 m^2/s condition, the water seepage of Combination 20 is 4.95 m^3/h, which is the maximum value for this condition; under the q = 0.6 m^2/s condition, the water seepage of Combination 24 is 6.95 m^3/h, which is the maximum value for this condition; under the q = 0.9 m^2/s condition, the water seepage of Combination 24 is 7.64 m^3/h, which is the maximum value for this condition. In summary, when q = 0.3 m^2/s, 0.6 m^2/s, 0.9 m^2/s, the corresponding optimal structural parameter combinations are Combination 20, Combination 24, Combination 24, respectively.

Table 9. Statistical table of water infiltration for combinations of structural parameters that meet the requirements for use.

No.	q = 0.3 m^2/s (kg/m^3)	q = 0.6 m^2/s (kg/m^3)	q = 0.9 m^2/s (kg/m^3)
Combination 6			5.00
Combination 10		4.92	5.74
Combination 11	3.23	4.28	4.99
Combination 12	4.12	5.37	6.17
Combination 13	3.84	4.93	5.71
Combination 14	3.74	4.83	5.62
Combination 15	3.26	4.15	4.81
Combination 16	3.87	4.97	6.51
Combination 17	3.57	4.35	5.43
Combination 18	3.13	4.10	4.82
Combination 19	3.71	4.74	5.28
Combination 20	4.95	6.11	6.80
Combination 21	3.37	4.52	4.94
Combination 22	3.90	5.12	5.90
Combination 23	4.30	6.00	6.56
Combination 24	4.85	6.95	7.64
Combination 25	4.07	5.10	5.95

When the measured runoff data and sediment data of the proposed water intake river section are known, we can optimize the combination of structural parameters of the artificial percolation water intake riverbed according to the above discriminative results, in order to meet the requirement that the sediment does not fall in the vortex tube silt and at the same time to obtain a larger volume of water intake, and improve the economic efficiency. If the natural flow of the river is slow, we can narrow the width of the river to achieve the single-width flow we need. If the natural longitudinal slope of the river is small, we can also build a dam to raise the bottom of the river to meet our needs. Therefore, the above discriminative results are of great significance for the practical application of the artificial percolation water intake riverbed.

7. Conclusions

The main conclusions of this paper are as follows:

1. The combination of structural parameters has an important effect on the vortex tube mean circumferential flow rate V_r and vortex tube water seepage volume Q. Different combination numbers represent different combinations of structural parameters, and each combination number presents different vortex tube mean circumferential flow rates and vortex tube water seepage. It can also be seen that the single-width flow rate has an important effect on the vortex tube mean circumferential flow rate V_r and vortex tube water seepage volume Q.
2. According to the results of the range analysis and ANOVA, different structural parameters have different degrees of influence on the mean circumferential flow rate of the vortex tubes V_r and the vortex tube seepage volume Q. With the change in flow conditions, the impacts of the vortex tube opening rate Ω on the vortex tube mean circumferential flow rate change, and the impacts of different structural parameters on the vortex tube seepage Q change greatly. The longitudinal slope of artificial riverbed i has the largest and most significant effect on the mean circumferential flow rate of the vortex tube, and each structural parameter has a certain effect on vortex tube seepage volume Q, but it does not reach a significant level.
3. When the sand content of the water flow is 15 kg/m^3 and the maximum sand grain size of the suspended mass is 2 mm, the optimal structural parameter combinations of the artificial riverbed under different working conditions are as follows: Combination 20 is the optimal structural parameter combination when q = 0.3 m^2/s; Combination 24 is the optimal structural parameter combination when q = 0.6 m^2/s; and Combination 24 is the optimal structural parameter combination when q = 0.9 m^2/s. These optimal combinations of structural parameters in certain water flow sand content conditions can ensure the sediment does not fall in the vortex tube silt, but can also obtain a larger amount of water seepage, as well as better economic efficiency.

8. Prospect

The optimization of various structural parameters in the artificial percolation riverbed holds significant importance for advancing the practical application of this technology. By adjusting the structural parameters of the artificial percolation riverbed, tailored solutions can be achieved to meet diverse water intake requirements across different river sections, irrespective of the current river topography. This adaptability offers a promising resolution to existing challenges in sandy river water intake technologies. Furthermore, our investigation into this novel method of water extraction and sand removal in sandy rivers is still in its exploratory phase. Further research is essential to explore the hydraulic characteristics of two-phase flow within artificial percolation riverbeds and to understand the impact of water extraction and sand removal in these riverbeds under two-phase flow conditions.

Author Contributions: Data curation, Y.L.; Funding acquisition, X.S.; Investigation, M.Y.; Resources, L.Z.; Software, L.W.; Supervision, X.S.; Validation, L.W.; Writing—original draft, M.Y.; Writing—review and editing, X.S. All authors have read and agreed to the published version of the manuscript.

Funding: This research was funded by the National Natural Science Foundation of China (Grant No. 51179116) and the Natural Science Foundation of Shanxi Province (Grant No. 202303021211141).

Data Availability Statement: This research was supported by the Collaborative Innovation Center of New Technology of Water-Saving and the Secure and Efficient Operation of Long-Distance Water Transfer Project at Taiyuan University of Technology.

Acknowledgments: This research was supported by the Secure and Efficient Operation of Long-Distance Water Transfer Project at Taiyuan University of Technology.

Conflicts of Interest: Author Lianle Wang was employed by China Railway 18th Bureau Group Co., Ltd. The remaining authors declare that the research was conducted in the absence of any commercial or financial relationships that could be construed as a potential con-flict of interest.

References

1. Zhang, M.B. Experimental Study and Application of Percolation Characteristics of Riverbed Sand and Pebble Media. Doctor's Thesis, Taiyuan University of Technology, Taiyuan, China, 2013.
2. Zhang, M.B.; Fan, G.S.; Zheng, Y. Experimental study on the technical parameters of artificial filter bed for Yellow River water containing mud. *J. Hydraul. Eng.* **2013**, *44*, 444–450.
3. Wang, Q.X. Experimental study and application of spiral flow sand discharge. *Sediment Res.* **1990**, *2*, 63–70.
4. Tiwari, N.K.; Sihag, P. Prediction of trapping efficiency of vortex tube. *ISH J. Hydraul. Eng.* **2018**, *26*, 59–67. [CrossRef]
5. Nan, J.H.; Gao, H.; Wang, C.Q. Experimental study and numerical simulation of a new type of cyclone sand discharge channel. *Adv. Eng. Sci.* **2022**, *54*, 116–123.
6. Wang, H.S.; Liu, Z.W. Research status and development trend of precipitation process. *Copp. Eng.* **2004**, *1*, 54–56.
7. Qiu, X.Y. Research on a new type of water-sand separation device. *J. Xinjiang Agric. Univ.* **2007**, *30*, 68–70.
8. Yang, S.D.; Qu, Z.Y.; Zhang, W.F. Experimental study on anti-clogging of drip irrigation with inorganic adsorbent treatment of Yellow River water. *J. Drain. Irrig Mach Eng.* **2020**, *38*, 517–522.
9. Giulia, D.S.; Camillo, N.; Antonio, C. The hydraulic separator Multidune: Preliminary tests on fluid-dynamic features and plastic separation feasibility. *Waste Manag.* **2008**, *28*, 1560–1571.
10. Floriana, L.; Monica, M.; Lorenzo, C. Separation of plastic waste via the hydraulic separator Multidune under different geometric configurations. *Waste Manag.* **2012**, *32*, 1306–1315.
11. Chen, W.M.; Zhe, P.G.; Gang, R. Application of membrane separation technology in the treatment of leachate in China: A review. *Waste Manag.* **2021**, *121*, 127–140. [CrossRef]
12. Tao, H.F.; Qiu, X.Y. Numerical simulation of flow field inside water-sand separation gill. *Trans. Chin. Soc. Agric. Eng.* **2013**, *29*, 38–46.
13. Fan, C.L.; Bai, X.F.; Liu, X.N. Research on the sand discharge law of vortex tube water flow. *Adv. Eng. Sci.* **1990**, *4*, 21–26.
14. Wang, Q.X. Experiment on the formation of spiral flow and sand discharge effect. *Yellow River* **1987**, *5*, 12–17.
15. Atkinson, E. Vortex-tube sediment extractors: I, Trapping efficiency. *J. Hydraul. Eng.* **1994**, *120*, 1110–1125. [CrossRef]
16. Atkinson, E. Vortex-tube sediment extractors: II, Design. *J. Hydraul. Eng.* **1994**, *120*, 1126–1138. [CrossRef]
17. Zhang, K.Q.; Liu, H.F. Development and Prospect of Vortex Tube Sand Discharge Technology Research. *Adv. Sci. Tech. Water Res.* **2000**, *2*, 16–18+69.
18. Zhao, T.; Li, L.; Mu, Z.W. Experimental study on water-sand separation in a large-scale turbid water hydraulic separation clear water device. *J. Sichuan Univ. Eng. Sci. Ed.* **2014**, *46*, 47–53.
19. Li, L.; Qiu, X.Y. Numerical simulation of weakly rotating flow in a clear water device for hydraulic separation of turbid water. *J. Hydroelectr. Eng.* **2008**, *2*, 103–109.
20. Keshavarzi, A.R.; Gheisi, A.R. Trap efficiency of vortex settling chamber for exclusion of fine suspended sediment particles in irrigation canals. *Irrig Drain.* **2006**, *55*, 419–434. [CrossRef]
21. Zhang, P.F.; Deng, S.H.; Qiu, Z.Y. Characterization of flow field of liquid-liquid dynamic cyclone. *Min. Mach.* **2007**, *4*, 63–66+5.
22. Cui, B.Y. Numerical Experimental Study of Hydrocyclone Flow Field and Separation Process. Doctor's Thesis, Northeastern University, Shenyang, China, 2014.
23. Li, L.; Wang, P.Y.; Wu, Y.F. Influence of overhanging plate opening on the flow field characteristics of sand discharge funnel. *Adv. Water Sci.* **2020**, *31*, 927–935.
24. Nan, J.H.; Wang, C.Q.; Li, W. Experiment on sand discharge characteristics of cyclone drainage channel. *Trans. Chin. Soc. Agric. Eng.* **2022**, *38*, 127–135.
25. Nan, J.H.; Dai, J.L.; Li, W. Study on the influence of body shape parameters on water and sand characteristics in cyclone drainage channels. *Adv. Sci. Tech. Water Res.* **2024**, *44*, 64–72.
26. Yang, M.; Li, Y.; Sun, X.; Wang, L. Numerical Simulation Study of an Artificial Percolation Riverbed and Its Hydraulic Characteristics under Different Reynolds Numbers. *Water* **2024**, *16*, 2791. [CrossRef]
27. Quan, H.; Guo, Y.; Li, R.N.; Su, Q.M.; Yi, C. Optimization design and experimental study of vortex pump based on orthogonal test. *Sci. Prog.* **2020**, *103*, 0036850419881883. [CrossRef]

28. Nan, J.H.; Luo, H.; Kangning, M.A.; Huan, G. Orthogonal numerical test method and application for body shape optimization of cyclonic sand discharge channels. *J. Hydroelectr. Eng.* **2022**, *41*, 160–169.
29. Wang, Y.; Huo, X. Multiobjective optimization design and performance prediction of centrifugal pump based on orthogonal test. *Adv. Mater. Sci. Eng.* **2018**, *2018*, 6218178. [CrossRef]
30. Chen, J.; Zheng, Y.; Zhang, L.; He, G.; Zou, Y.; Xiao, Z. Optimization of geometric parameters of hydraulic turbine runner in turbine mode based on the orthogonal test method and CFD. *Energy Rep.* **2022**, *8*, 14476–14487. [CrossRef]
31. Liu, F.; Wang, C.; He, J.L. Experimental study on optimization of twisted nosecan body shape based on orthogonal design. *South-to-North Water Transf. Water Sci. Technol.* **2020**, *18*, 166–175.
32. Zhang, C.; Yan, H.; Jamil, M.T.; Yu, Y. Improvement of the flow pattern of a forebay with a side-intake Pumping station by diversion piers based on orthogonal test method. *Water* **2022**, *14*, 2663. [CrossRef]
33. Shen, Z.H.; Wang, C.; Zhang, J.; Qiu, S. Study on Part-Load Cavitation in High-Specific-Speed Centrifugal Pump. *Water* **2024**, *16*, 2180. [CrossRef]
34. Yang, S.Q.; Tan, S.K.; Wang, X.K. Mechanism of secondary currents in open channel flows. *J. Geophys. Res. Earth Surf.* **2012**, *117*, F04014. [CrossRef]
35. Zhang, K.Q. A preliminary study on the flow structure and sand discharge mechanism of spiral flow. *J. Shihezi Univ. Nat. Sci.* **1984**, *1*, 1–6.
36. Zhang, Y.; Liu, J.; Zhang, Y.Z. Analytical study of spiral flow formation and its flow structure at the bottom of a canal. *China Rural Water Hydropower* **2009**, *11*, 53–55+57.
37. Liu, R.J.; Zhang, Y.W.; Wen, C.W. Research on orthogonal experimental design and analysis methods. *Lab. Technol. Manag.* **2010**, *27*, 52–55.
38. Fei, X.J. Sand-holding capacity and sand transport characteristics of suspended-mass flows. *Sediment Res.* **2003**, *3*, 30–34.
39. Dou, G.R. Revisiting the sediment starting flow rate. China Water Resources Society. In Proceedings of the 2001 Annual Conference of the China Water Resources Society, Beijing, China, 30–31 October 2001.

Disclaimer/Publisher's Note: The statements, opinions and data contained in all publications are solely those of the individual author(s) and contributor(s) and not of MDPI and/or the editor(s). MDPI and/or the editor(s) disclaim responsibility for any injury to people or property resulting from any ideas, methods, instructions or products referred to in the content.